Spotting Of Glaucoma Using A Minimal Approach With Ternary Level Convolutional Neural Network

A.Padma[1], Dr.M.Sivajothi[2], Dr.M.Mohamed Sathik[3]

[1]Research Scholar, Research Centre for Computer Science, Sadakathullah Appa College, Tirunelveli, Tamilnadu, India.

[2]Associate Professor, Dept. of Computer Science, Sri Parasakthi College for Women, Manonmaniam Sundaranar University, Tirunelveli, Tamil Nadu, India.

[3]Former Principal, Sadakathullah Appa College, Manonmaniam Sundaranar University, Tirunelveli, Tamil Nadu, India

Abstract:

Glaucoma is an eye disease that leads to vision loss by causing damage to the optic nerve. A novel method namely Tripartite Tier Convolutional Neural Network Scheme (TT_CNN Scheme) was proposed for detection of glaucoma. The proposed model contains three layers namely left tier, middle tier and right tier. This model is designed in such a way that shows improved result. Multiple .classifiers are used for classifying the fundus images as normal or glaucomatous images. Random Forest Classifier shows improved results than other classifiers. This TT_CNN Scheme has been analysed using MIAG RIMONE (Release2) database and MIAG RIMONE (Release3) database and obtained result is compared with the results of LP_LDS method. The performance metrics illustrates enhanced results for TT_CNN Scheme than LP_LDS method

DOI: 10.24297/j.cims.2023.7.7

1. Introduction

Glaucoma [1] is an eye disease that causes the loss of vision. Recent studies suggested that glaucoma is the third leading cause for blindness. In India around 12 million people are affected. To avoid such blindness, many techniques were proposed to detect the presence of glaucoma. Among them, CNN [2] is one of the approach that shows better accuracy. It reduces the human intervention as it extracts the features directly from the images. It is widely used in many applications such as object classification, speech recognition, pattern recognition and more.

2. Related Work

Prasad N. Madhure [3] proposed a technique for Optic Disc (OD) and Optic Cup (OC) segmentation in which adaptive histogram equalization and gabor filters are used as a key feature to classify the super pixel as disc or non-disc pixel. Simple Linear Iterative Clustering (SLIC) algorithm is implemented for super pixel generation. The cup-to-disc [4] (CDR) ratio is calculated to classify the retinal images as glaucomatous or healthy.Gilbert Lim [5] presented a method to segment OD and OC and the blood vessels are removed from OD using inpainting.Sukanya [6] proposed a technique for OD segmentation. This process involves median filter for noise removal, Andy operator for edge detection, morphological operations for image enhancement and Support Vector machine classifier for classification. Tamilarasi [7] presented a work in which the RGB retinal image is converted into greyscale image using principal component analysis and the blood vessels are eliminated using mathematical functions. The OD is segmented using generalized distance function, stochastic watershed and geodesic transformation function. Vijaya R. Patil [8] implemented a technique where the input fundus image is resized and converted into greyscale image. Canny edge detection technique is used to find the edges and shapes. Finally the OD was located using circular hough transform.

Ali Mohamed Nabil Allam [9] presented a method in whi the fundus image was converted into L*a*b colorspace to decompose the chromocity information of the image. Based on the information of unsupervised k-means algorithm, the fundus image was partitioned into five disjoint clusters. The image with intense portion was selected. The threshold value was computed using statistic based metrics. The image with relative brightness was preserved. Finally the OD was identified from the threshold image.Jenitta [10] presented a feature extraction approach in which the texture features in the medical images are extracted using Local Pattern Descriptor(LPD) and Gray Level Co-occurence Matrix (GLCM). Local Mesh Co-occurence Pattern (LMCoP) was constructed from the fusion of local mesh pattern with GLCM and Local Vector Co-occurence Pattern (LVCoP) was generated from the fusion of local vector pattern with GLCM. For further feature extraction, the combination of LMCoP and LVCoP was implemented.Loretta chim [11] presented a method based on adaptive local texture analysis with different features. These features are acquired from co-occurence matrix, the fractal dimension and blood density. Retinal images are decomposed into patches using sliding box method. By applying pre processing techniques, regions with different intensities and sound are obtained. A method which is the combination of voting scheme and sorting procedure was implemented to identify the OD.

Raghavendra U[12] implemented an artificial neural network (autoencoder) and trained to snub noise. Darvish [13] proposed a multistage methodology to detect exudate from the fundus images. Shuang Yu [14] presented a methodology for neovascularisation detection using machine learning. Cheng Wan [15] proposed a technique for feature extraction. Several layers included in neural network are trained for the localization of optic disc region. The candidate pixels in the OD region was arranged based on threshold value. The center of gravity among the pixels are computed and the OD region was identified for the detection of glaucoma. Qaisar Abbas[16] presented a deep belief network approach to get more deep discriminative features for the diagnosis of glaucoma. Sevastopolsky [17] presented a technique to distinguish OD and OC using U-Net convolutional neural network.

Kamble [18] proposed a method to identify glaucoma. A classifier model was utilized to find the edges of OD region. The edges found in the color or grayscale image was converted to binary image for analysis. The Circle hough transform method is used for feature extraction and to locate the OD region accurately. Mamta Juneja [19] stated a methodology in which two neural networks are functioning concurrently to split OD and OC to identify the eye disease.
Andres Diaz-Pinto [20] presented a new method in which the retinal image was synthesized and a approach to diagnose glaucoma anchored in Deep Convolutional Generative Adversarial Networks. Shanshan Tu [21] proposed a novel model that comprise two phases namely optic disc localization and Glaucoma Diagnosis Network (ODG Net). In the first phase, the prominent field is extracted by means of saliency map and is combined with CNN model for rapid and low cost OD localization. The isolated OD portion is further provided to deep learning models to recognize glaucomatous and non-glaucomatous images.

Aniket Patil [22] implemented a technique for glaucoma detection using Convolutional Neural Network. The input image is preprocessed through Gaussian blur by removing noise and then fed to CNN model. The preprocessed input image acts as an input layer. In convolution layer, feature maps are generated by applying filters on the input image. The ReLU activation function performs threshold operation for each input variable with values less than zero. The pooling layer reduces the spatial size of images. The same operations are performed in such a way to produce down sampled data. The obtained features are flattened as a column vector and given as an input to fully connected layer where it is classified as healthy or affected eye. H. N. Veena [23] presented a novel technique for OD and OC segmentation to diagnose glaucoma using deep learning CNN. The deep learning CNN technique is individually modelled for segmentation of OD and OC. Thirty nine layers are involved in this process for major feature extraction and error reduction during training time. The image resolution is maintained using down sampling and up sampling techniques which improves the accuracy of OD and OC segmentation. After the detection of OD and OC region, CDR is calculated to determine whether the input retinal image is normal or glaucomatous.

3. Methodology

CNN OVERVIEW

The CNN comprises layers such as

- Input layer
- Convolution layer
- ReLU layer
- Max Pooling layer
- Fully Connected layer
- Softmax layer
- Classification layer

Input Layer

The foremost input tier captures the unprocessed input image with three dimensions. It converts the image into lower dimension without losing its characteristics. For example, if the height and width of the image is 15, then the depth is represented as 1 for grayscale and 3 for RGB. It is shown as 15 ×15 × 1 for grayscale and 15 × 15 × 3 for RGB. The three dimensional matrix of the image is converted into a single column as 225 × 1. If there are ***n*** training samples, then the dimension of input will be (225, ***n***).The outcome of the first layer will be fed to the successive layer as an input.

Convolution Layer

Whenever a convolution is applied to an image, the size of the image is reduced and the information is condensed into an individual pixel.

If the image size is n × n, and filter size is f × f, then the resultant image after convolution will be

$$(n \times n) * (f \times f) = (n - f + 1) \times (n - f + 1)$$

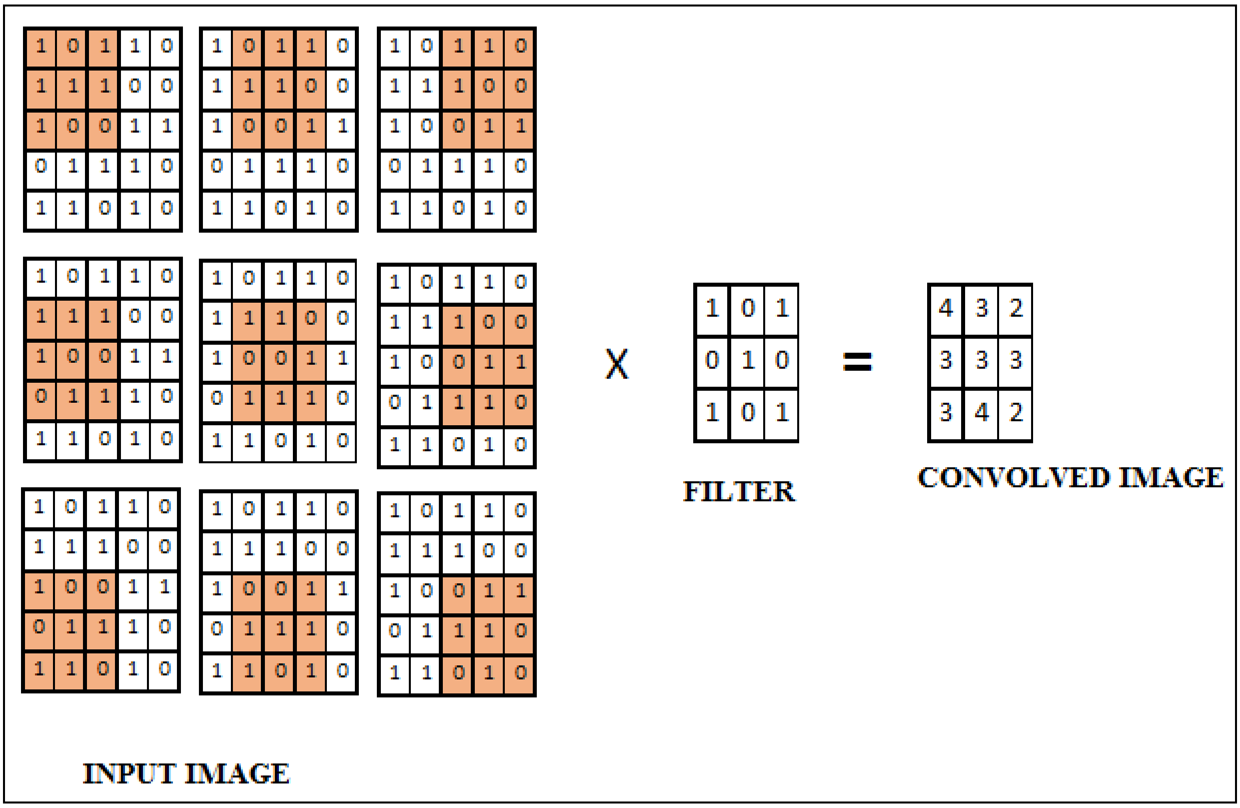

Figure 1 Convolved Image after convolution

ReLU layer (Rectified Linear Unit)

A nonlinear activation function is applied to achieve non-linear operation on each element and provide output as rectified feature map by ignoring non positive values. The output of relu layer is expressed as

$$g(y) = \max(0, y) \qquad (3)$$

Where y is non negative value

In other words, if the range of any element is less than 0, then it can be set as 0, otherwise retaining the same. Since only the positive input values are retained, the speed of the training dataset is accelerated and it is also faster than other activation functions.

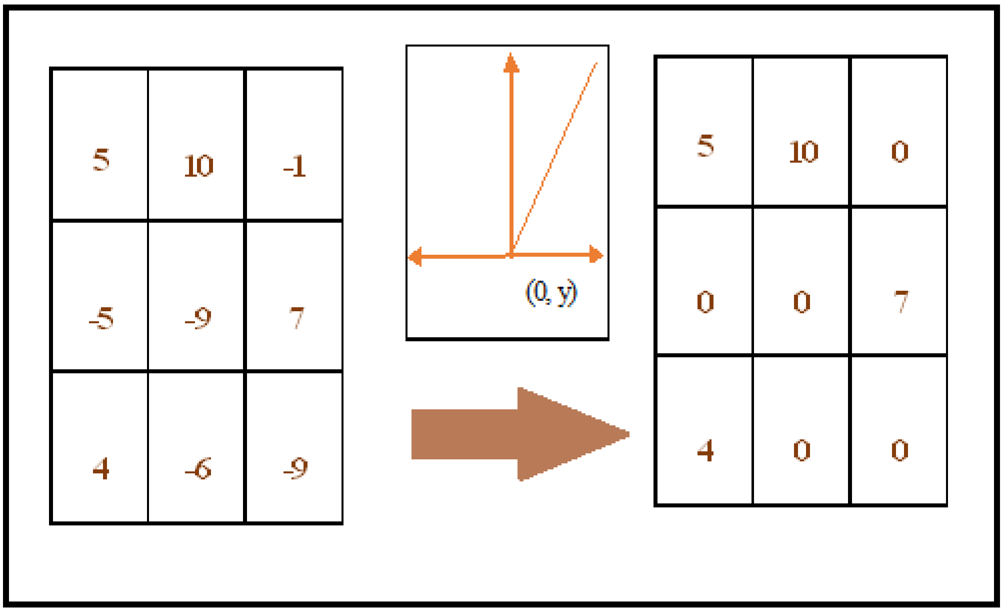

Figure 2 ReLU operation

Pooling layer

The spatial size of convolved image is lessened using this layer. It progresses rapid computation and restricts overfitting. The different types of pooling are

- Max pooling
- Average pooling
- Sum pooling

The sampling rate of the input is dropped by parting it into sub regions and the value is calculated to maintain the vital information. Max pooling displays the maximum value in the feature map. Average pooling represents the average of the values in the feature map.Sum pooling shows the sum of the values in the feature map.

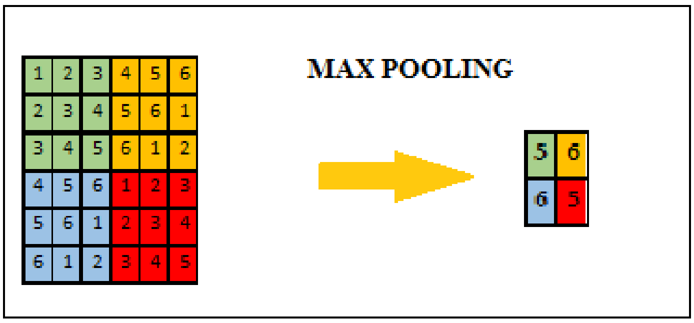

Figure 3 Max Pooling

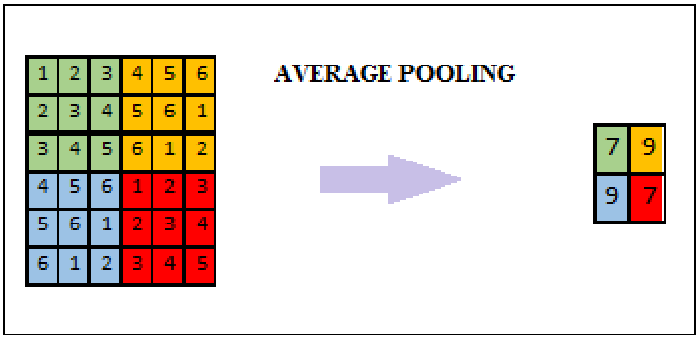

Figure 4 Average Pooling

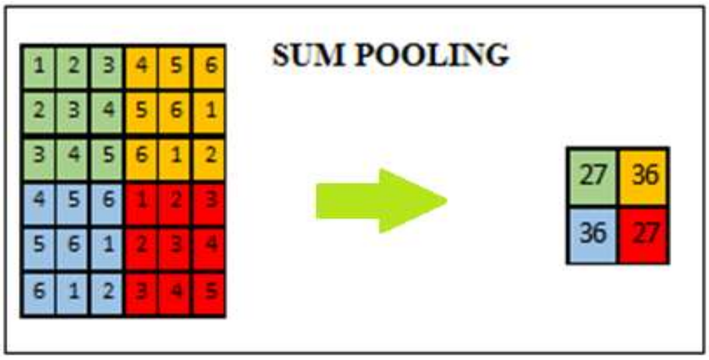

Figure 5 Sum Pooling

Fully connected layer

The matrix values are constricted into column vector and it is fed into a fully connected layer.

SoftmaxLayer

Softmax function is implemented for the classification of outputs based on the number of classes. It is used for classification of numerous classes.

$$f(y_i) = \frac{e^{Y_i}}{\sum_{j=0}^{k} e^{Y_j}} \qquad (4)$$

Y is the vector of raw outputs from the neural network where i=0,1,2,......k and j=0,1,2,........k.

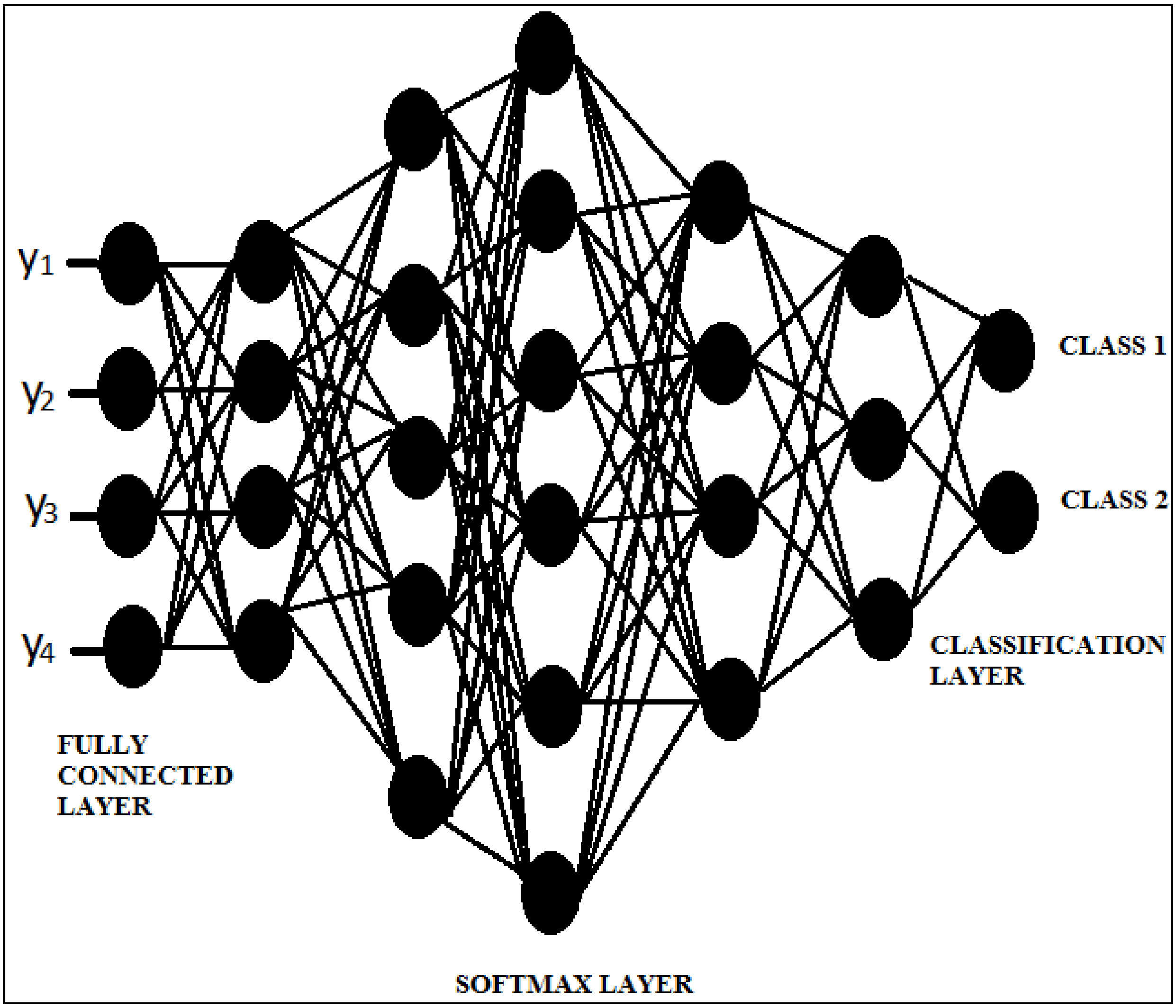

Figure 6 Output Layer

TRIPARTITE TIER CNN ARCHITECTURE

In TT_CNN, each input image is passed through a sequence of convolution layers along with pooling, fully connected layers, filters. The Soft-max function is used to classify the image with probabilistic values 0 and 1.

The RGB fundus image is taken as input for TT_CNN model and is normalized. It is then fed to the three tier of convolution layer. In convolution layer, *a 3x3x1 convolved features is obtained by convoluting a 64 x 64x1 image with a 3x3x1 kernel (filter). Similarly 5x5x1and 7x7x1 convolved features are obtained by convoluting a 64 x 64x1 image with a 5x5x1 kernel and 7x7x1 respectively. Multiple convolution* continues until very deep layers are extracting most important features.

The convolved output image is then shifted to relu layer which is an activation function that ignores the negative values.The Pooling layer reduces the spatial size of the Convolved Feature. Reduction of the number of features improves the performance of the model by removing irrelevant or redundant information. Lower-dimensional data requires less storage and computational resources, making it faster and more efficient to process. Dimensionality reduction leads to easier interpretation and analysis.

Stride is the count of pixels that can be hovered over the input matrix. When the stride is equal to 1, then the filters are moved to 1 pixel at a time and similarly, if the stride is equal to n, then the filters are moved to n pixels at a time. Max pool of size 2 and stride 2 is utilized to extract more deep features.

The resultant matrix value is flattened as single column vector value and each vector from three tiers are merged and fed to fully connected layer. Then the softmax function calculates the proportion of the exponential of the input value and the aggregate of exponential values which ranges between 0 to 1.

Finally classification layer shows the final output based on the class probability.

Table 1 Layer Structure for TT_ CNN

OVERALL LAYER STRUCTURE		
LEFT LAYER	MIDDLE LAYER	RIGHT LAYER
Input fundus image with dimension 224x224x3		
conv_1 (64 filters with 3x3) and Relu_1	conv_5 (64 filters with 5x5) and Relu_5	conv_3 (64 filters with 7x7) and Relu_3
conv_2(64 filters with 3x3) and Relu_2	conv_6(64 filters with 5x5) and Relu_6	conv_4 (64 filters with7x7) and Relu_4
MaxPool_2 (pool size 2 and Stride 2)	MaxPool_6(pool size2 and Stride 2)	MaxPool_4 (pool size 2 and Stride 2)
conv_8(64 filters with 3x3) and Relu_8	conv_7(64 filters with 5x5) and Relu_7	conv_9(64 filters with 7x7) and Relu_9
MaxPool_3 (pool size 2 and Stride 2) Relu_11	MaxPool_1 (pool size2 and Stride 2) Relu_10	MaxPool_5 (pool size 2 and Stride 2) Relu_12
Dropout_2	Dropout_1	Dropout_3

fc_2 (output size 100)	fc_1 (output size 100)	fc_3 (output size 100)
CONCATENATION LAYER		
fc_4 (output size 2)		
SOFTMAX LAYER		
CLASSIFICATION LAYER		

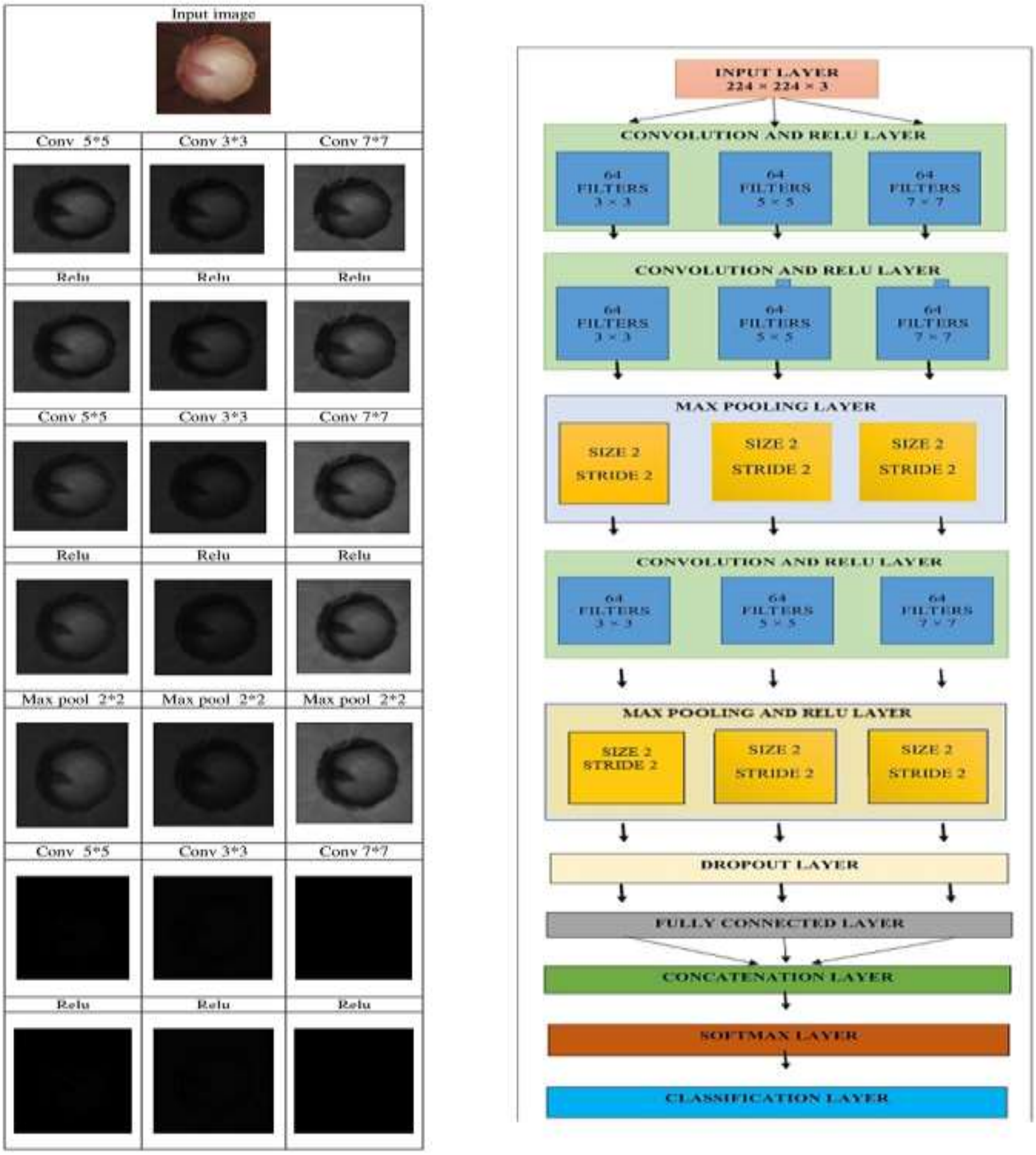

Figure 7 TT_CNN Architecture with feature map

4. Experimental Results And Analysis

The existing LP_LDS [24] and proposed TT_CNN [25] methods were implemented on MIAG RIM ONE release2 (255 normal images and 200 glaucomatous images) and release 3 datasets (85 normal images and 39 glaucomatous images) and their performance were shown below in the Table1. For both datasets, 70% of images were trained and 30% were considered for testing.

Table 3 Performance metrics for MIAG RIM ONE release2 and release3 datasets using LP_LDS and TT_CNN methods

	Dataset	Classifier	Accuracy	Sensitivity	Specificity	Precision	Recall	Fscore
Existing LP_LDS Method	MIAG RIMONE Release2	SVM	0.7206	0.713	0.713	0.7187	0.7130	0.7144
		RF	0.8971	0.8929	0.8929	0.8992	0.8929	0.8952
		KNN	0.6985	0.6976	0.6976	0.6962	0.6996	0.6965
		DT	0.8162	0.815	0.815	0.8141	0.815	0.8145
	MIAG RIMONE Release3	SVM	0.5806	0.481	0.481	0.4762	0.4810	0.4730
		RF	0.6774	0.5262	0.5262	0.5948	0.5948	0.4833
		KNN	0.4516	0.3595	0.3595	0.3510	0.3595	0.3550
		DT	0.5806	0.481	0.481	0.4762	0.4810	0.4732
Proposed TT_CNN Method	MIAG RIMONE Release2	SVM	0.9926	0.9919	0.9919	0.9933	0.9919	0.9926
		RF	0.9926	0.9926	0.9926	0.9928	0.9926	0.9926
		KNN	0.9779	0.9779	0.9779	0.978	0.9779	0.9779
		DT	0.9706	0.9706	0.9706	0.971	0.9706	0.9706
	MIAG RIMONE Release3	SVM	0.982	0.979	0.979	0.982	0.979	0.98
		RF	0.991	0.986	0.986	0.994	0.986	0.99
		KNN	0.964	0.96	0.96	0.961	0.96	0.96
		DT	0.955	0.94	0.94	0.959	0.94	0.948

Case	Actual Images	Predicted outcome

ositive	Glaucomatous	Glaucomatous
FalsePositive	Healthy	Glaucomatous
False Negative	Glaucomatous	Healthy
True Negative	Healthy	Healthy

Table 1 Confusion matrix for glaucoma detection

Accuracy

It is an instinctive metric used to measure the functioning of the methods and it is a ratio of perfectly identified observations to the total observations. Its ability is to differentiate the patient and healthy cases. It significantly shows how near the predicted value comes to its actual value.

$$.\boldsymbol{Accuracy} = \frac{\boldsymbol{True\ Positives+True\ Negatives}}{\boldsymbol{True\ Positives+False\ Positives+True\ Negatives+False\ Negatives}} \qquad \textit{Equation1}$$

Accuracy is calculated as the sum of True positives and True Negatives to the sum of True Positives, False Positives, True Negatives and False Negatives.

Overfitting was one of the problem occurred in CNN when accuracy stops improving after certain number of epochs. Minimization of overfitting was the significant reason for the better performance of RF classifier rather than other classifiers.

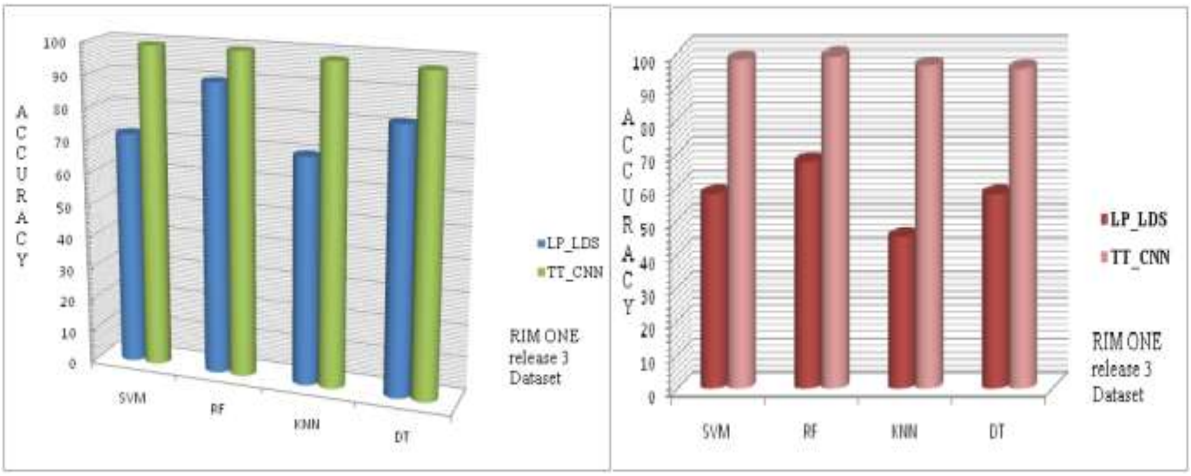

Figure 8 Accuracy for LP_LDS and TT_CNN method using classifiers

From Figure3 it was found that TT_CNN method shows better accuracy value than LP_LDS by 27.2% for SVM, 9.55% for RF, 27.94% for KNN and 15.44% for DT in MIAG RIM ONE release2 dataset. Also TT_CNN method shows better accuracy value than LP_LDS by 40.14% for SVM, 31.36% for RF, 51.24% for KNN and 37.44% for DT in MIAG RIM ONE release3 dataset.

Specificity

It reveals the proportion of healthy persons diagnosed correctly as healthy.

$$\boldsymbol{Specificity} = \frac{\boldsymbol{True\ Negative}}{\boldsymbol{True\ Negative + False\ Positive}} \qquad \textit{Equation 2}$$

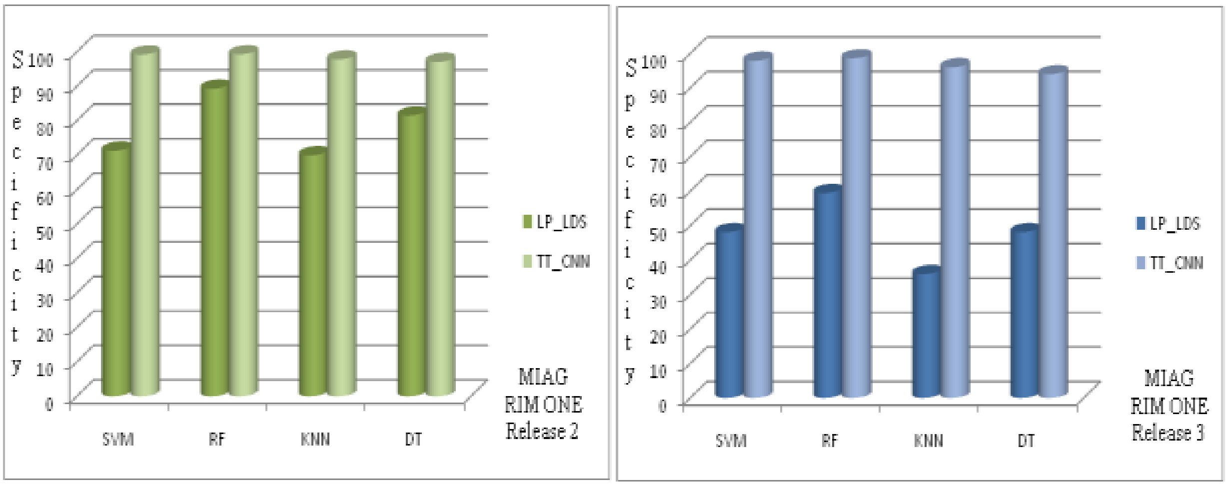

Figure 9 Specificity for LP_LDS and TT_CNN method using classifiers

From Figure5 it was observed that TT_CNN method shows better specificity value than LP_LDS by 27.89% for SVM, 9.97% for RF, 27.83% for KNN and 15.56% for DT in MIAG RIM ONE release2 dataset. Also TT_CNN method shows better specificity than LP_LDS by 49.8% for SVM, 39.12% for RF, 60.05% for KNN and 45.9% for DT in MIAG RIM ONE release3 dataset.

Recall or Sensitivity

It is the number of correct positive predictions to the number of entire glaucomatous images. Recall is the measure of completeness. Usually during medical analysis the model was proposed in such a way to obtain output sensitive predictions. To avoid labelling glaucomatous as healthy, high recall was needed for glaucomatous prediction.

$$\boldsymbol{Recall} = \frac{\boldsymbol{True\ Positive}}{\boldsymbol{True\ Positive + False\ Negative}} \qquad \textit{Equation 3}$$

It was important that recall consider the wrong predictions. In convolutional neural network, a proper loss function was assigned that is sensitive to changes. The key aspect was to fix the threshold value that is to be assigned to the final layer of CNN. To obtain maximum recall, the threshold value was set below 0.5. i.e., around 0.2

It was found that RF classifier was well suited for large dataset as it has low variance value.

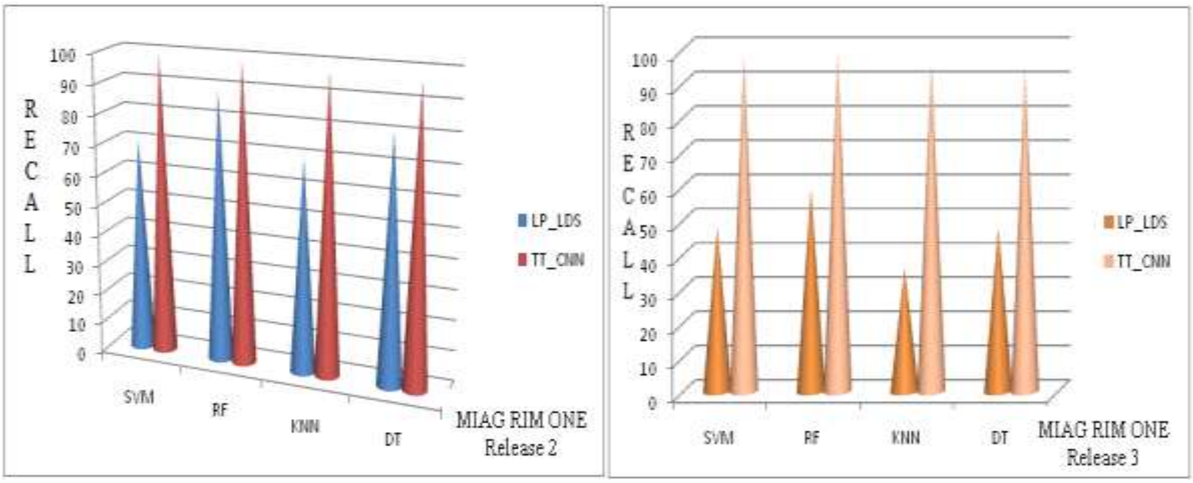

Figure 10 Recall for LP_LDS and TT_CNN method using classifiers

From the results it was found that the values of recall and specificity remain the same. From Figure6 it was observed that TT_CNN method shows better recall value than LP_LDS by 27.89% for SVM, 9.97% for RF, 27.83% for KNN and 15.56% for DT in MIAG RIM ONE release2 dataset. Also TT_CNN method shows better recall than LP_LDS by 49.8% for SVM, 39.12% for RF, 60.05% for KNN and 45.9% for DT in MIAG RIM ONE release3 dataset.

5. Conclusion

The performance of existing LP_LDS method and proposed TT_CNN method were implemented on MIAG RIM ONE release2 and release3 datasets and their performance were compared. The results of TT_CNN technique was found to be excellent than LP_LDS approach based on various aspects. Among four classifiers, Random Forest classifier exhibited better outcome than other classifiers. As a whole it was also found that all the classifiers perform well for a large dataset (MIAG RIMONE release2) than the other.

References

1. https://www.nei.nih.gov/learn-about-eye-health
2. https://towardsdatascience.com/convolutional-neural-networks
3. Prasad N. Maldhure, Prof.V.V Dixit,' Glaucoma Detection Using Optic Cup and Optic Disc Segmentation' , International Journal of Engineering Trends & Technology, Vol.20, Issue 2, pp. 52-55, 2015.
4. https://www.aao.org/education/image/cup-disc-ratio
5. Gilbert Lim ,Yuan Cheng, Wynne Hsu, Mong Li Lee,' Integrated Optic Disc and Cup Segmentation with Deep Learning' , ICTAI '15 Proceedings of the 2015 IEEE 27th International Conference on Tools with Artificial Intelligence, pp. 162-169, 2015.
6. Sukanya. R, Ganga Holi,' Energy Efficient Routing Algorithms for Mobile Ad Hoc Networks–A Survey' , International Journal of Computer Science Engineering, Vol.4, Issue 3, pp. 102-109, 2015.
7. Tamilarasi, Duraiswamy, ' Ensemble System for Optic Disc and Macula Detection' , International Journal of Advanced Research in Computer
8. Engineering & Technology, Vol.3, Issue 1, pp. 228-232, 2014.
9. Vijaya R. Patil, Vaishali Kumbhakarna, Dr. Seema Kawathekar, ' Detection of Optic Disc in Retina using Digital Image Processing' , International Journal of Computer Techniques, Vol.2, Issue 1, pp. 20-23, 2015.
10. Ali Mohamed Nabil Allam, Aliaa Abdel-Halim Youssif and Atef Zaki Ghalwash, "Segmentation of Exudates via Color-Based K-Means Clustering and Statistical-based Thresholding, Journal of Computer Science, DOI: 10.3844/jcssp.2017.524.536,October 2017.
11. Jenitta1 & R. Samson Ravindran, "Image Retrieval Based on Local Mesh Vector Co-occurrence Pattern for Medical Diagnosis from MRI Brain Images" , Image & Signal Processing, August 2017.
12. Loretta Ichim and Dan Popescu, "Optic Disc Localization Based on Feature Sorting" , Publishing House of the Romanian Academy, 2016.
13. Raghavendra U , Anjan Gudigar, Sulatha V. Bhandary,Tejaswi N Rao, "A Two Layer Sparse Autoencoder for Glaucoma Identification with Fundus Images" , Journal of Medical Systems , DOI: 10.1007/s10916-019-1427-x, July 2019.
14. J. Darvish and M. Ezoji, "Morphological Exudate Detection in Retinal Images using PCA-based Optic Disc Removal" , Journal of AI and Data Mining Vol 7, No 4, DOI: 10.22044/JADM.2019.1488, 2019.

15. Shuang Yu , Di Xiao , Yogesan Kanagasingam, "Machine Learning Based Automatic Neovascularization Detection on Optic Disc Region" , IEEE Journal of Biomedical and Health Informatics , Volume: 22 , Issue: 3 , May 2018.
16. Xu P., Wan C., Cheng J., Niu D., Liu J. (2017) Optic Disc Detection via Deep Learning in Fundus Images. In: Cardoso M. et al. (eds) Fetal, Infant and Ophthalmic Medical Image Analysis. OMIA 2017, FIFI 2017. Lecture Notes in Computer Science, vol 10554. Springer, Cham.
17. Qaisar Abbas, " Glaucoma-Deep: Detection of Glaucoma Eye Disease on Retinal Fundus Images using Deep Learning" , International Journal of Advanced Computer Science and Applications, Vol. 8, No. 6, 2017.
18. Sevastopolsky. "A Optic disc and cup segmentation methods for glaucoma detection with modification of U-Net convolutional neural network" , Pattern Recognition and Image Analysis, volume 27, pages 618–624, 2017.
19. Seema Tukaram Kamble, S.A.Patil, "Automatic Detection of Optic Disc using Structural Learning" , International Journal of Engineering Research & Technology (IJERT), ISSN: 2278-0181, IJERTV7IS050091, Vol. 7 Issue 05, May-2018.
20. Juneja, M., Singh, S., Agarwal, N. et al. Automated detection of Glaucoma using deep learning convolution network (G-net). Multimed Tools Appl , https://doi.org/10.1007/s11042-019-7460-4 , 2019.
21. A. Diaz-Pinto, A. Colomer, V. Naranjo, S. Morales, Y. Xu and A. F. Frangi, "Retinal Image Synthesis and Semi-Supervised Learning for Glaucoma Assessment," in *IEEE Transactions on Medical Imaging*, vol. 38, no. 9, pp. 2211-2218, Sept. 2019
22. Jahanzaib Latif, Shanshan Tu,Chuangbai Xiau, "ODGNet: a deep learning model for automated optic disc localization and glaucoma classification using fundus images,SN Applied Sciences, https://doi.org/10.1007/s42452-022-04984-3, March 2022
23. Aniket Patil,Risha Shetty, "Glaucoma Detection using Convolutional Neural Network" , IRJET,Vol 7 Issue:01, Jan 2020
24. H. N. Veena, A. Muruganandham, T. Senthil Kumaran, " A novel optic disc and optic cup segmentation technique to diagnose glaucoma using deep learning convolutional neural network over retinal fundus images" , Journal of King Saud University- Computer and Information Sciences, https://doi.org/10.1016/j.jksuci.2021.02.003, 2021

25. Padma, A., Sivajothi, M. and Sathik, M.M., "Glaucoma Detection Using Little Wood Paley Decomposition On Local Derivative Structure Of Fundus Images". European Journal of Molecular & Clinical Medicine, 7(10), p.2020.
26. Padma, A., Sivajothi, M. and Sathik, M.M., "A Contemporary Strategy for the Recognition of Glaucoma with Tripartite Tier Convolutional Neural Network". Annals of the Romanian Society for Cell Biology, pp.883-898, 2021